CIRCULATION OF AIR MASSES IN THE UPPER ATMOSPHERE DURING THE IQSY

I. B. Biybosunov, K. A. Karimov

ABSTRACT. Results of measurements made during the period 1964-1965 are presented.

Ionospheric Wind Conditions

One of the basic tasks of making radar observations of meteors during /3* the International Year of the Quiet Sun (IQSY) was the study of the principles of air mass movement in the meteor zone, since the investigation of upper atmosphere circulation is of great significance in solving a number of problems in geophysics and in the mastery of space. Beginning in June 1964, regular monthly measurements were made of the drift velocity of meteor trails at altitudes from 80 to 110 km, at Frunze in the Radiometeor Laboratory of the Institute of Physics and Mathematics, using a specially designed radar installation.

This article describes some results of measurements made during 1964-1965.

The radar equipment used for the experiment had the following fundamental parameters: carrier frequency f = 39.5 MHz, transmitter pulse power P_u = 30-50 kW, radar pulse repetition frequency F = 100-200 pps, main pulse width τ = 8-10 μsec, receiver sensitivity $\alpha = (3\text{-}5)\cdot 10^{-14}$ W. Reception and transmission were by separate five-channel antennas of the "wave channel" type (two antennas, supplied in-phase) raised to a height of $h = \lambda/2$ above the earth's surface. The receiving and transmitting antennas were 100 to 150 meters apart. A detailed description of the installation is given in reference [1].

Measurements were made in two directions according to a special IQSY program over a six to eight day period in the last ten days of each month. During this time winds in the south-north and west-east directions were studied. North (N) and east (E) were taken as positive.

---

* Numbers in the margin indicate pagination in the foreign text.

The signals reflected from the meteor trails were recorded on motion picture film, running continuously in front of the screens of cathode ray tubes. Signals were intensified upon arrival of a meteor echo. /4

The radial component of meteor trail drift velocities based on Doppler periods, determined from the photography,

$$V_r = \lambda/2T_g$$

was found. Here λ is the radar wavelength, and T_g is the period of phase fluctuation in signals reflected from the trail.

The direction of trail displacement was determined by mixing the Doppler signal phases (lead or lag) in two phase channels of a detector. The voltage was supplied to the second phase detector with a phase shift of 90°.

Ionospheric winds in the meteor zone were assumed to be horizontal with an accuracy within a few degress [2]. The horizontal components of the drift velocity were calculated by using the formula

$$V = V_r/\cos\Theta ,$$

from which Θ, the angle of elevation of a reflecting point on the meteor trail, was found as

$$\Theta = \text{arc}\sin(h_{char}/R),$$

where

R is the slant range to the trail;

h_{char} is the mean characteristic altitude, in our case equal to 93 km.

From 2000 to 5000 values of drift velocities were obtained for each direction. Hourly values of the horizontal velocity components were averaged over several days in each direction. Thus, the number of combined values ranged from 30 to hundreds per hour. The more reliable results were obtained during the night and morning hours, when the number of recorded meteors was at a maximum.

The mean hourly wind velocity values obtained were subjected to harmonic analysis, the results of which are listed in Table 1. Each equation in the table contains four terms: a constant term, characterizing the preferred /6

wind direction, a 24-hour, a 12-hour, and an 8-hour component. Amplitudes of higher harmonics (6-4 hours) are smaller as compared to the second and first, and can be ignored in the second approximation. We described our wind measurement procedures in reference [3].

TABLE I *

Month	Direction	Type of equation
		1964
June	N—S	3,5+ 7,4 Sin 15 (t+ 3,5)+19,7 Sin 30 (t+ 7,5) + 2,7 Sin 45 (t+4,2)
	E—W	0,8+ 4,5 Sin 15(t+20,6)+15,9 Sin 30 (t+ 5,6) + 7,3 Sin 45 (t+4,7)
August	N—S	16,3+25,1 Sin 15 (t+ 4,1)+ 7,1 Sin 30 (t+ 6,5) + 9,8 Sin 45 (t+3,3)
	E—W	11,2+18,3 Sin 15 (t+ 9,4)+28 Sin 30 (t+ 6,0) + 2,0 Sin 45 (t+1,2)
September	N—S	4,8+ 9,7 Sin 15 (t+16,7)+16,4 Sin 30 (t+11,6) + 13,0 Sin 45 (t+5,7)
	E—W	14,2+11,5 Sin 15 (t+ 2,0)+18,7 Sin 30 (t+ 7,0) + 8,4 Sin 45 (t+3,0)
October	N—S	—2,8+ 1,9 Sin 15 (t+12,0)+17,7 Sin 30 (t+10,0) + 4,2 Sin 45 (t+1,0)
	E—W	19,8+12,2 Sin 15 (t+ 4,8)+14,7 Sin 30 (t+ 7,1) + 13 Sin 45 (t+2,4)
November	N—S	4,5+13,2 Sin 15 (t+ 4,1)+ 9,6 Sin 30 (t+ 8,6) + 2,8 Sin 45 (t+7,4)
	E—W	15,6+ 7,5 Sin 15 (t+15,8)+ 8,2 Sin 30 (t+ 6,6) + 8,9 Sin 45 (t+ 4,5)
December	N—S	15,0+13,9 Sin 15 (t+ 4,5)+17,8 Sin 30 (t+ 7,4) + 12,2 Sin 45 (t—1,4)
	E—W	2,1+ 5,6 Sin 15 (t+19,8)+25,1 Sin 30 (t+ 4,2) + 1,3 Sin 45 (t+0,4)

* Commas represent decimal points.

Let us review the results of ionospheric wind velocities individually for each year. In 1964, the investigations were conducted in June, but technical reasons prevented ionospheric wind velocities from being measured in July.

Figure 1 and Table 1 show drift histograms and list their corresponding equations for 1964, from which it will be seen that the amplitudes of the 24-hour components vary differently for different months, from A_1 = 2 m/sec to A_1 = 25 m/sec; those of the 12-hour components vary from A_2 = 7 m/sec to A_2 = 28 m/sec.

The preferred direction is east for the west-east component in the prevailing wind, with the maximum air mass transport velocity 20 m/sec.

The zonal components of the prevailing vectors are directed towards the north.

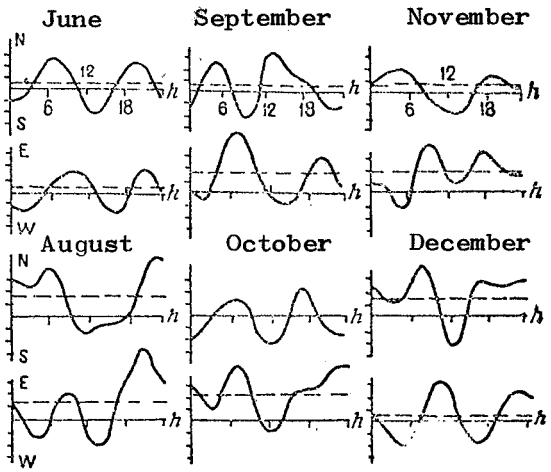

Figure 1. Histograms of meteor trail drifts for 1964.

Figure 2 shows the polar diagrams of changes in the vectors of the 24-hour, 12-hour, and 8-hour components over a 24-hour period.

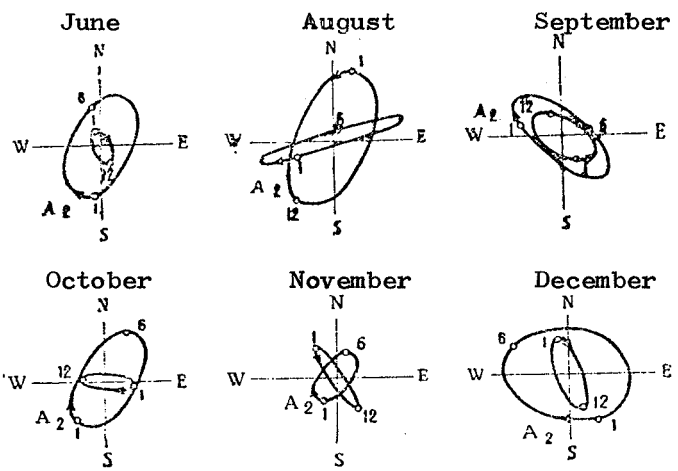

Figure 2. Polar wind diagrams for 24-hour and 12-hour components.

The rotation of the vector of the 12-hour component is clockwise. /7
The 24- and 8-hour components have no general behavior patterns.

Thus, in the given latitude for the place (the coordinates of the range in which the SOM-1 radar was located in Frunze were $\varphi = 72°35'$, $\iota = 42°56'$), at altitudes of 80-110 km, a large stream of air is transported primarily to

the east relative to the earth, at an average velocity of the order of 30 m/sec.

Let us review the experimental data obtained by the SOM-1 radar in 1965.

Figure 3 shows histograms of meteor trail drifts for January through December, inclusive.

Measurements were made for six to eight days on the days indicated in the IQSY program. Lines calculated using the harmonic analysis method and taking three harmonics into consideration are shown solid. The equations for all the curves for 1965 are listed in Table 2.

Analysis of the equations shows that the most significant harmonic is the 12-hour, with maximum amplitude A_2 = 20 m/sec.

The amplitude of the 24-hour harmonic is a maximum of A_1 = 16 m/sec.

The amplitudes of the 12-hour and 24-hour harmonics have a seasonal variation, with maximum values occurring during the summer.

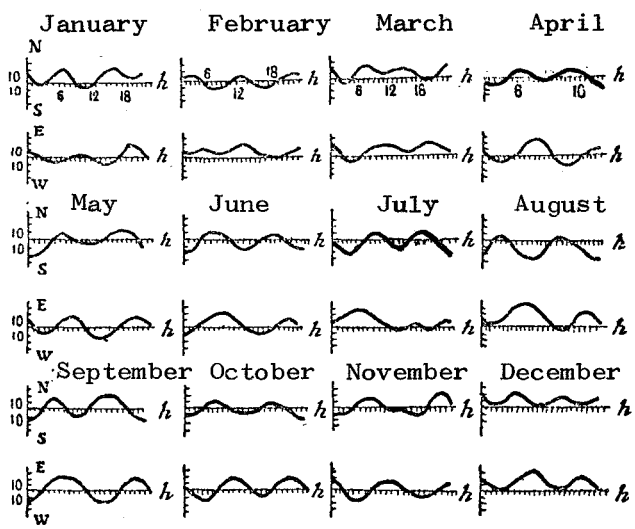

Figure 3. Histograms of meteor trail drifts for 1965.

The ratio of mean amplitudes of 12-hour to 24-hour harmonics for meteor altitudes is /8

$$K = (\overline{A}_2/\overline{A}_1) \simeq 3$$

The amplitude of the 8-hour harmonic is of the order of the 24-hour harmonic amplitude and has no seasonal variations.

Figure 4 shows the polar diagrams of the rotation of the vector for the 24- and 12-hour harmonics for analyzing the phase relationships of the zonal and meridional components. The 24-hour component vector experiences no regular changes during the year. Clockwise, as well as counterclockwise, rotation is observed. The 12-hour harmonic vector rotates clockwise throughout the year, except in March and July.

The polar diagrams for the 12-hour components show that in fact the northern component always leads to the east, as distinct from the 3-hour component.

The 12-hour wind component is directed largely northward 0600 throughout the year.

TABLE 2 *

Month	Direction	Type of equation
		1965
January	N—S	10,0+ 6,0 Sin 15 (*t*+ 7,5)+11,0 Sin 30 (*t*+ 8,5) + 9,0 Sin 45 (*t*+ 2,2)
	E—W	0,5+ 9,2 Sin 15 (*t*+ 6,4)+10,8 Sin 30 (*t*+ 4,2) + 4,6 Sin 45 (*t*+ 5,8)
February	N—S	—2,4+ 5,0 Sin 15 (*t*+ 4,6)+ 9,5 Sin 30 (*t*+ 3,1) + 5,0 Sin 45 (*t*+ 6,8)
	E—W	7,5+ 4,0 Sin 15 (*t*+20)+ 7,1 Sin 30 (*t*+ 2,1) + 1,9 Sin 45 (*t*+ 3,8)
March	N—S	8,0+ 5,1 Sin 15 (*t*+20)+ 4,5 Sin 30 (*t*+ 5,4) +12 Sin 45 (*t*+ 2,4)
	E—W	7,9+ 9,1 Sin 15(*t*+13)+ 8,9 Sin 30(*t*+ 4,8) + 3,7 Sin 45 (*t*+ 0,7)
April	N—S	—0,4+10,0 Sin 15 (*t*—17,4)+16,0 Sin 30 (*t*+ 8,2) + 4,7 Sin 45 (*t*+ 6,3)
	E—W	—2,1+5,6 Sin 15 (*t*+1,2)+11,0 Sin 30 (*t*+ 4,6) + 5,5 Sin 45 (*t*+ 2,8)
May	N—S	—5,8+11,0 Sin 15 (*t*+15,6)+12,8 Sin 30 (*t*+ 7,4) + 6,3 Sin 45 (*t*+ 4,4)
	E—W	0,5+ 2,1 Sin 15 (*t*+23,1)+16,2 Sin 30 (*t*+ 5,6) + 4,6 Sin 45 (*t*+ 1,0)
June	N—S	—6,0+ 5,0 Sin 15 (*t*+17,0)+14,3 Sin 30 (*t*+ 8,2) + 8,9 Sin 45 (*t*+ 4,1)
	E—W	3,0+11,7 Sin 15 (*t*+22,2)+18,2 Sin 30 (*t*+ 6,9) + 4,2 Sin 45 (*t*+ 6,5)
July	N—S	—8,0+ 7,9 Sin 15 (*t*+13,1)+20,3 Sin 30 (*t*+ 7,3) +11,0 Sin 45 (*t*+ 0,5)
	E—W	11,0+16,1 Sin 15 (*t*+23,9)+13,4 Sin 30 (*t*+ 7,1) + 4,4 Sin 45 (t+ 2,8)
August	N—S	—17,6+2,3 Sin 15 (*t*+12,3)+16,7 Sin 30 (*t*+10,7 +3,2 Sin 45 (*t*+ 6,5)
	E—W	17,6+15,2 Sin 15 (*t*+23,0) +21,5 Sin 30 (*t*+ 5,4) + 7,8 Sin 45 (*t*+ 5,2)
September	N—S	3,0+ 8,9 Sin 15 (*t*+15,8)+15,6 Sin 30 (*t*+ 9,4) + 12,1 Sin 45 (*t*+ 4,9)
	E—W	—2,0+ 5,8 Sin 15 (*t*+ 2,9)+ 7,4 Sin 30 (*t*+ 7,5) + 5,6 Sin 45 (*t*+ 3,0)
October	N—S	—5,1+ 3,8 Sin 15 (*t*+21,6)+10,7 Sin 30 (*t* 9,0) + 4,8 Sin 45 (*t*+ 5,5)
	E—W	0,9+ 1.3 Sin 15 (*t*+ 7,2)+21,3 Sin 30 (*t*+ 4,9) + 3,6 Sin 45 (*t*+ 6,3)
November	N—S	—1,6+ 1,6 Sin 15 (*t*+21,0)+13,5 Sin 30 (*t*+ 5,4) + 6,3 Sin 45 (*t*+ 4.6)
	E—W	—0,8+ 3,4 Sin 15 (*t*+19,2)+14,8 Sin 30 (*t*+ 3,0) + 5,4 Sin 45 (*t*+ 1,6)
December	N—S	14,2+ 2,6 Sin 15 (*t*+ 5,8)+4,7 Sin 30 (*t*+ 8,7) + 9,0 Sin 45 (*t*+ 2,3)
	E—W	11,0+ 6,1 Sin 15 (*t*+ 2,2)+12,5 Sin 30 (*t* + 5,4) + 5,7 Sin 45 (*t*+ 7,1)

* Commas represent decimal points.

Regular changes do not occur in the 8-hour component vector.

These results agree in general with those obtained by the Khar'kov group [4, 5].

Analysis of the prevailing wind for the north and east components for 1964 and 1965 (Figure 5) reveals that the meridional component (E - W) is primarily directed eastward, with maximum amplitude in the summer and winter months A_0 = 12 m/sec. The minimum amplitude occurs in the spring-fall months.

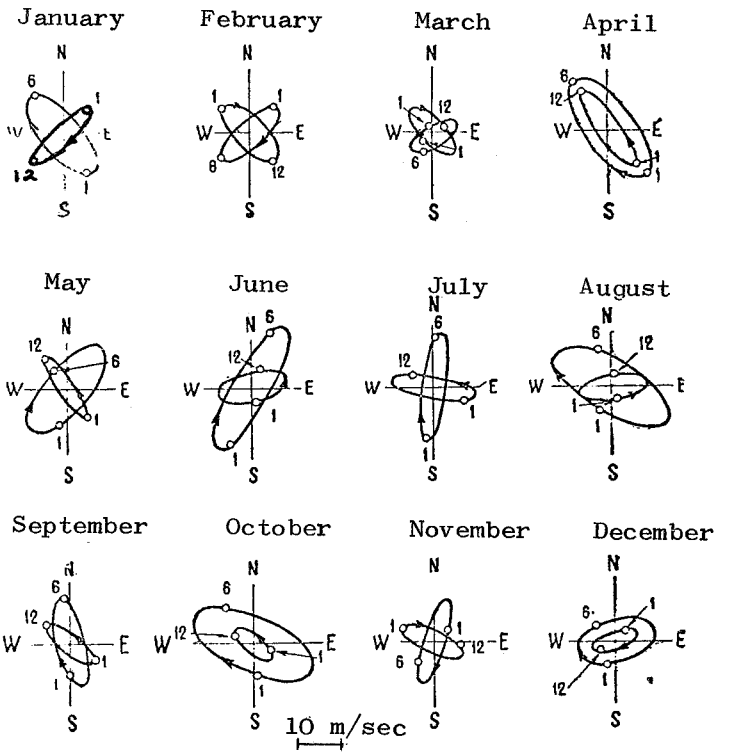

Figure 4. Polar diagrams of 24-hour and 12-hour component vectors.

Characteristic of the zonal (N-S) component in the summer months is the transport of the air masses in a southerly direction, with the maximum velocity 10 m/sec. /11

There is a change in vector direction in the spring-fall months; movement of the air masses is toward the pole.

The difference in temperatures in the upper atmosphere over the polar and equatorial regions affects the zonal component.

The southern component should predominate in the summer months.

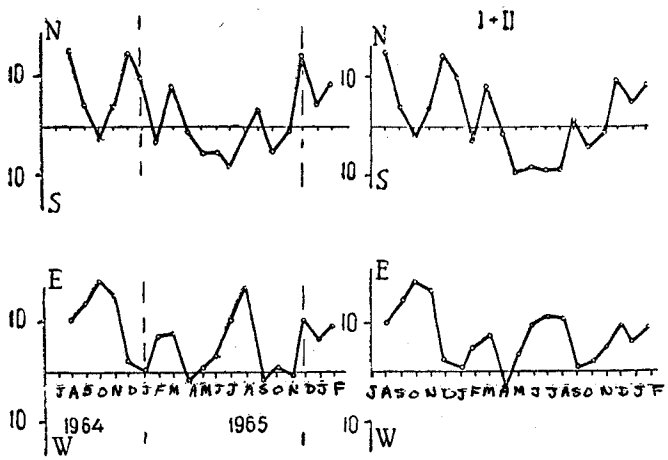

Figure 5. Prevailing wind direction, 1964-1965.

Temperature gradients, as well as the effect of the earth's rotation, caused by kinematic viscosity, and equal to the ratio

$$\eta/\rho$$

where η is the coefficient of friction, and ρ is density of the atmosphere at the corresponding altitude [6], affect the wind direction in the meridional region.

The results fit the model of atmospheric circulation on a global scale suggested by A. Kochanski [7] in 1963 quite well.

It should be pointed out that the 1965 data on atmospheric circulation are more reliable.

The presence of a significant amplitude in the 12-hour harmonic indicates the resonant nature of atmospheric oscillations at these altitudes. The presence of a cold region with a temperature minimum at altitudes of the order of 95 km, that is, the presence of temperature troughs in the atmosphere along the vertical, leads to the occurrence of free atmospheric oscillations with a period of 12 hours. /12

Thus, the effect of the semidiurnal solar gravitational force increases because of the resonance of the atmosphere at these altitudes.

The resonance theory was suggested by Wilkes [8] and developed in detail by White [9].

In conclusion, it should be noted that questions of atmospheric circulation at altitudes above 80 km require further detailed study, and year-to-year comparisons.

Annual Cycle of Turbulence Intensity

The kinetic energy of turbulent motions in a unit mass

$$I = 1/2\ (\overline{U'x}^2 + \overline{U'y}^2 + \overline{U'z}^2),$$

where $U'_i = U_i - \overline{U}_i$ is the pulsation, or the turbulent velocity, and i is the component of the measured value of the velocity in the specified direction, can be taken as the turbulence intensity.

The distribution of pulsation velocities at a fixed point must be close to normal (Gaussian). In the case of radio meteor measurements, the velocity values depend on different points within a volume bounded by the width of the antenna radiation pattern and the thickness of the meteor layer.

What follows from the theory of turbulence is that turbulent energy is defined by the density gradient, $d\rho/dz$, which has a seasonal pattern, and by the mean wind gradient, which affects temporal changes in turbulence intensity.

Turbulence intensity was calculated for each hour, using the formula:

$$I = 1/2\ (\overline{U'x}^2 + \overline{U'y}^2)$$

when there were no vertical pulsation velocities. It should be pointed out that $\overline{U'z}^2$ may increase by 15-30% and distort the value of the overall intensity.

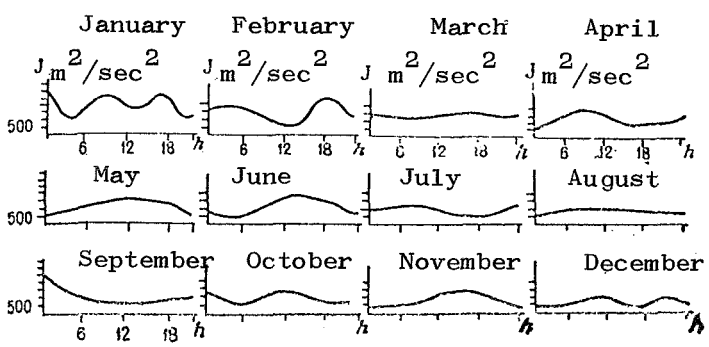

Figure 6. Diurnal changes in turbulence intensity in 1965.

Figure 6 shows the diurnal changes in intensity for the 12 months of 1965, and for January 1966. There is a daily pattern for some months (January, May, June, November) with a maximum with a mean error of $\sigma J = 400\ m^2/sec^2$ during the daytime, but a tendency toward a maximum during the night hours is characteristic of other months (February, April, September). There was no behavior pattern to be observed for the other months, i.e. the vector of pulsation intensity is constant throughout the 24 hours. Solar corpuscular radiation probably is the responsible factor for this effect. /13

The processing of wind data must include the daily J pattern when there are daily changes in J.

Figure 7 shows the annual turbulence intensity pattern for 1965.

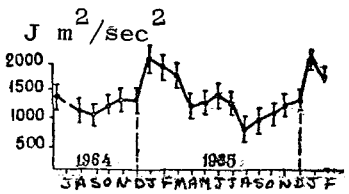

Figure 7. Seasonal change in turbulence intensity.

An annual pattern, with an intensity minimum during the summer ($J = 710\ m^2/sec^2$ in August) and an intensity maximum during the winter ($J = 2400\ m^2/sec^2$), will be seen quite clearly. The mean error in J is of the order of $\sigma J = 200\ m^2/sec^2$. The data on annual change is turbulence intensity concord with the results obtained by the Kazan group, and can be explained by the different effects of the Archimedean forces in the summer and winter [10].

Time Constant and the Horizontal Scale for Strong Vortices

It is believed that irregular motions in the meteor zone are the result of the turbulization of the laminar air streams produced by forces of hydrodynamic origin. Experience shows that the wind velocity, measured in layers several kilometers apart in altitude, sometimes differs by tens of meters per second. This indicates the presence of a turbulent wind gradient. The mean value of the turbulent wind gradient, according to /14

reference [11], is

$$\text{gradU} = dU/dh = 8.5 \text{ m/sec per km.}$$

The fundamental parameters characterizing turbulent motion are the rate of arrival of energy, ε, from outside sources, the pulsation velocity, U', for large-scale vortices, the size of the vortices, L, and the lifetime of the vortices, T.

The procedure for estimating the quantities U', L, and T has been given by Greenhow and Neufeld [12], as well as by Delov, Lagutin, and Lysenko [11]. The values found were U' = 28 m/sec, T = 110 min, and L = 180 km.

The authors did the work of evaluating the influence of U', L, and T in the heart of continental Asia and of comparing these magnitudes with those found earlier. The evaluation was made using the preceding procedure (an autocorrelation function was calculated from pulsation velocities averaged for 30-minute intervals, with a limited range sample for 24-hour intervals) of the form

$$R(T) = \frac{\sum_{t=1}^{n} U(t) \cdot \sum_{t=1}^{n} U(t+\tau)}{\left[\sum_{t=1}^{n} U^2(t) \cdot \sum_{t=1}^{n} U^2(t+\tau)\right]^{1/2}}; \quad \tau = 0,1,\ldots n,$$

as well as G. Teptin's procedure [10]. The autocorrelation function was calculated for a fixed point of the form

$$R(T) = \frac{\sum_{t=1}^{n} U'(\bar{r},t) \sum_{t=1}^{n} U'(\bar{r},t+\tau)}{\left[\sum_{t=1}^{n} U'^2(\bar{r},t) \sum_{t=1}^{n} U'^2(\bar{r},t+\tau)\right]^{1/2}}; \quad \tau = 0,1,\ldots,n,$$

where U'($\bar{r}$, t) is the turbulent velocity at the fixed point with coordinates $\bar{r}$ at time t. In addition to the autocorrelation function for the point, the autocorrelation for shower meteors was calculated (for a statistical check). /15

The number of meteors drops significantly when the radiation pattern is narrowed because the single-point meteor radar method does not permit measuring small-scale turbulence characteristics. The characteristics of turbulent motion change during extended radar observations so it is necessary to confine the measurements to the streams. At the same time, the majority of the reflecting points lie in a single plane, the echo plane, which passes through the radar perpendicular to the direction of the radiant. In this case there is no need to measure the azimuths of the angles of reflection when calculating the specular reflection, and the selection of the work area for averaging can be made out to radar range. In our case, the horizontal area had a maximum limit of 30 km. $\Delta R \leq 30$ km. Altitudes were determined with respect to the coefficient of ambipolar diffusion, $D = f(h)$

$$\lg D = 0.067 \cdot h - 5.6 .$$

The scatter of altitude points was $\Delta h = \pm 3$ km, using Greenhow's method [14].

Reflecting points in the altitude interval $\Delta h \leq 8$ km then were selected. Thus, the size of the region was contained in an area $\Delta R \leq 30$ km and $\Delta h \leq 8$ km.

The following streams were used to evaluate the characteristics:

21 - 22 October 1965 (Orionids)

16 - 17 November 1965 (Leonids)

2 - 3 January 1966 (Quadrantids)

The autocorrelation function was calculated in unit values of pulsation velocities for two to three hour time intervals (Figure 8).

The autocorrelation function transition time, T_0, at "zero" characterizes the time constant for strong vortices. The heterogeneity lifetime, /16 determined in unit values for the "point," is

$$\tau_0 = 30 \text{ min} \quad \text{(Orionids)}$$
$$\tau_0 = 25 \text{ min} \quad \text{(Quadrantids)}$$

Correspondingly, $T = \tau_0$, calculated for a sporadic background over a 24-hour interval for averaged 30-minute interval velocities, is

τ_0 = 80 min (22 October 1965);

τ_0 = 70 min (3 January 1966).

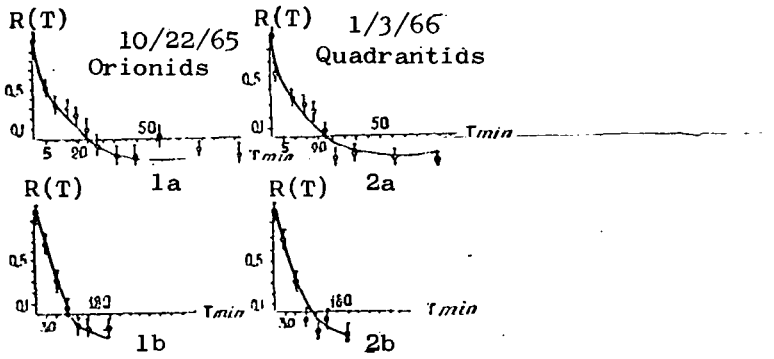

Figure 8. Autocorrelation function curves. 1a, 2a - in unit values; 1b, 2b - 30 minute averages.

The evaluation of the horizontal dimensions of strong vortices was made using the formula

$$L_r = (\overline{U}'^2)^{1/2} \cdot \tau_0$$

for known $\overline{U}'$ and τ_0 for the streams

L_r = 36 km - October (Orionids);

L_r = 30 km - January (Quadrantids).

The sizes of the nonuniformities for the sporadic meteors case for a 24-hour period, averaged for 30-minute intervals, were

L_r = 80 km - October;

L_r = 120 km - January.

In our opinion, a size of the order of 30-36 km is more probable for large-scale vortices. /17

The results of the determination of τ_0 equal to 70-80 min are far too high because the component attributable to the presence of periodic wind components over a 24-hour period are superimposed on the exponential decrease in R(T), as well as to the influence of the antenna radiation pattern (influence of the region illuminated by the radar antenna). The question of the degree of influence exerted by the antenna radiation pattern is still unresolved. Attenuation of the autocorrelation function shows that fluctuations in wind velocity are a combination of fluctuations of a turbulent character and periodic oscillations with random amplitudes and phases.

The magnitudes α and β can be calculated during the approximation of the autocorrelation function by the expression

$$R(t) = R_0 \cdot e^{-\alpha \Delta t} \cos \beta \Delta t .$$

If $\beta > \alpha$, the periodic oscillations with random amplitudes and phases make a definite contribution to the spectral density of the velocity distribution at frequencies close to τ_0. If $\beta < \alpha$, the principal role in this process is played by velocity fluctuations of a turbulent character [15]. The autocorrelation function (see Figure 8; 1a and 2a) has the form

$$R(t) = R_0 \cdot e^{-0.11t} \cdot \cos 0.06t \text{ (Orionids)};$$
$$R(t) = R_0 \cdot e^{-0.12t} \cos 0.05t \text{ (Quadrantids)},$$

where wind velocity fluctuations of a turbulent character are of primary significance.

Analogous autocorrelation functions (see Figure 8; 1b and 2b) can be expressed by the equations

$$R(t) = R_0 \cdot e^{-0.18t} \cos 0.30t \text{ (Orionids)};$$
$$R(t) = R_0 \cdot e^{-0.15t} \cdot \cos 0.28t \text{ (Quadrantids)}.$$

The α and β relationship shows how significant are the effects of periodic wind fluctuations over a 24-hour period, leading as they do to an increase in the time of existence of discontinuity τ_0.

The magnitude of the time constant τ for large-scale vortices of the order of 25-30 min agrees with Teptin's recent data [10]. /18

The connection between time and space spectra is described by J. Taylor's hypothesis, and by the hypothesis of conservation of perturbation form without significant alterations when movement is along a straight line with air streams with mean stream velocity, by the so-called "frozen turbulence" hypothesis, which has been proven for small scales.

The fluctuations in hydrodynamic magnitudes at some point can be used to judge the pulsations along a straight line passing through this point in the direction of the mean wind. In fact, the turbulence field is not frozen, and its configuration undergoes temporal distortion. If the turbulent

energy is far less than the mean motion energy, the errors caused by using the "frozen turbulence" hypothesis to describe the structure of the turbulence field will be small. They will be significant when the energy of turbulent pulsations is commensurate with tne averaged motion energy. This hypothesis provides wind velocity values at one fixed moment in time for different points and for different moments in time. A structural function of the type

$$D_{rr}(r_*) = \overline{\Delta U^2}_r.$$

was calculated to evaluate the horizontal dimensions of "frozen" vortices.

Pairs of points at approximately the same altitude were grouped by distance between points found by the "frozen turbulence" hypothesis for a fixed moment in time. The differences in the horizontal velocity components were calculated for these points with the mean wind vector taken into consideration.

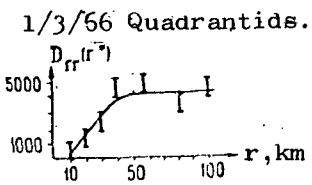

Figure 9. Structural function curve.

Figure 9 is the structural function, $D_{rr}(r_*)$, curve, plotted for the January Quadrantids, where we see that the horizontal turbulence scale is in the limits of 30-40 km. This dimension agrees with data for the autocorrelation function with respect to unit values for the Quadrantids and Orionids.

Thus, the correlation of velocities in "frozen turbulence" is seen to be in the limits of 30-40 km. These data agree with optical observations by Savrukhin and Gul'medov. /19

The rotation of individual clusters of meteor trails results in an increase in vortex size of the order of 20-50 km [16].

Conclusion

1. Observed during 1964-1965 in the upper atmosphere at altitudes of 80-115 km was the steady transport of air masses in a southeasterly direction; with mean velocities up to 15 m/sec in the summer.

What is primarily a northeasterly transport of the air masses is characteristic in the winter.

2. Mean wind values show changes in oscillation amplitude over a 24-hour period, with the most significant harmonic oscillations with a 12-hour period and an amplitude reaching 40 m/sec.

3. The magnitude of turbulence intensity has a clearly defined seasonal pattern, and is greater in the winter than in the summer by a factor of three.

4. Our assessment of the dimensions of large-scale nonuniformities indicates that the horizontal scale of the turbulence, or the radius of the correlation of drift velocities, is in the limits of 30-40 km.

REFERENCES

1. Karimov, K., Kostromin, V., Berezovskiy, M., "Radar Equipment for Observing Meteors in Kirghizia," Sb.: Meteornoye rasprostraneniye radiovoln [In collection: Meteor Propagation of Radio Waves], No. 3, Kazan', 1966.

2. Dokuchayev, V. P., "The Influence of Geomagnetic Disturbances of the Drift of Ionized Gas," Izv. VUZov, Radiofizika, No. 3, 1960.

3. Biybosunov, I., Karimov, K. A., "Wind Conditions in the Ionosphere Over Kirghizia," Sb.: Meteornoye rasprostraneniye [In collection: Meteor Propagation], 1966.

4. Kashcheyev, B. L., Lebedinets, V. N., "Radar Investigation of Meteor Phenomena," MGG, 7, 1961.

5. Lysenko, I. A., "Air Flows in the Meteor Zone from Radar Observation," Astronomicheskiy zhurnal, No. 21, 1963.

6. Mitra, S. K., Verkhnyaya atmosfera [The Upper Atmosphere], IL, 1959.

7. Kochanski, A., "Circulation and Temperatures at 70 to 100 kilometer Height," J. Geophys. Res., 68, 1963, 213.

8. Wilkes, M. V., Oscillations of the Earth's Atmosphere, Cambridge, 1949.

9. White, M., "Thermal and Gravitational Atmospheric Oscillations-Ionospheric Dynamo Effects Included," I. Atmos. Terr. Phys., 17, 1960, 3.

10. Zadorina, Pokrovskiy, Sidorov, Teptin, Fakhrutdinova, "Atmospheric Motion at Altitudes of 80-100 km from Radio Meteor Observations in Kazan'," Izv. AN SSSR, seriya fizika atmosfery i okeana, No. 1, 1967. /20

11. Delov, I., Lagutin, M., Lysenko, N., "Investigation of Certain Parameters of Turbulent Motion Using Radar Observation of Meteor Trails," Izv. VUZov, Radiofizika, Gorkiy, 1964.

12. Greenhow, J., Neufeld, E., "Measurement of Turbulence in the Upper Atmosphere," Proceeding Phys. Soc., 74, 1959.

13. Greenhow, J., Hall, I., "Diurnal Variations of Density and Scale Height in the Upper Atmosphere," J. Atmosphere Terr. Phys., Vol. 18, 1960, 205.

14. Pinus, Ye., "Energy Spectra of Pulsations in Wind Velocity in the Free Atmosphere," Meteorologiya i gidrologiya, No. 4, 1966.

15. Gul'medov, Kh., "Upper Atmosphere Turbulence from Optical Observations of Meteor Trails in Ashkhabad and Kazan'," Geomagnetizm i aeronomiya, Nos. 2, 3, 1963.